Published online November 3, 2005

6296–6307 *Nucleic Acids Research, 2005, Vol. 33, No. 19*
doi:10.1093/nar/gki946

Tracking of microinjected DNA in live cells reveals the intracellular behavior and elimination of extrachromosomal genetic material

Noriaki Shimizu*, Fumie Kamezaki and Shiho Shigematsu

Faculty of Integrated Arts and Sciences, Hiroshima University, 1-7-1 Kagamiyama, Higashi-hiroshima, 739-8521, Japan

Received September 1, 2005; Revised and Accepted October 18, 2005

ABSTRACT

We here addressed the basic question, how does extrachromosomal DNA behave when it is placed in the nuclear or the cytoplasmic environment and how is it eliminated? To do this, we tracked microinjected DNA molecules in live cells. In the cytoplasm, the diffusion of microinjected DNA was inhibited in a size- and linearity-dependent manner, probably by the intermediate filament. This was followed by the rapid disappearance of the DNA fluorescent signal. In the nucleus, the diffusion was also dependent on the size of the molecule and was accompanied by the aggregation of the DNA. The aggregation may be due to a putative DNA-binding molecule, whose level is high during the G_1 phase. Surprisingly, the injected DNA could move across the nuclear membrane and appeared in the cytoplasm, which suggests the presence of a transport system. The intracytoplasmic behavior and the elimination of such DNA was obviously different from the DNA that was directly injected at the cytoplasm. The DNA remaining in the nucleus appeared to be stable and persisted in the nucleus or, after cell division, in the cytoplasm, for more than one cell cycle. These findings provide a novel and basic understanding of the behavior and elimination of a wide variety of extrachromosomal genetic material.

INTRODUCTION

Many kinds of extrachromosomal genetic material can exist in mammalian cells. An example is viral nucleic acid. Furthermore, the artificial introduction of engineered DNA is commonly used for basic biology research and for industry or therapeutic purposes. Since such exogenous genetic material frequently perturbs the genomic information that dictates the integrity of an organism, most bacterial cells have restriction–modification systems that selectively destroy exogenous information. However, it is not known whether such elimination systems exist in higher eukaryotes, which is curious since it is probable that such systems are vital for protecting our genome from invading viral information. Moreover, such systems may decrease the efficiency of transformation with an artificial gene, which has obvious implications for gene therapy strategies in medicine.

In addition to exogenous genetic material, the cells from almost all normal mammalian tissues and cancer cells bear endogenous extrachromosomal closed circular DNA that is thought to be excised from the chromosome arm [for a review see ref. (1)]. In cancer cells, such submicroscopic episomes are thought to generate extrachromosomal double minutes (DMs) or a chromosomal homogeneously staining region (HSR), both of which are the cytogenetic manifestations of gene amplification [for reviews see refs (2,3)]. Indeed, a plasmid bearing a mammalian replication origin and a matrix attachment region mimics gene amplification in cancer cells as it efficiently generates DMs and HSR (4,5). As gene amplification plays a pivotal role in malignant transformation, a decrease in the copy number of amplified genes leads to the loss of malignant phenotypes, apoptotic death or cellular differentiation (6–10). The elimination of amplified genes may occur when they localize on extrachromosomal DMs, and it was mediated by the selective incorporation of DMs into the cytoplasmic micronuclei (11,12). The entrapment of acentric and autonomously replicating DMs into the micronuclei was caused by their unique intracellular behavior (13,14), especially their segregation into daughter cells by sticking to the mitotic chromosome in a manner called 'hitchhiking' [for a review see refs (15,16)]. Significantly, many viral nuclear plasmids are segregated by a similar hitchhiking mechanism during M phase (17–20). Therefore, the intracellular behavior and the elimination of these viral plasmids from the cell may be similar to that of DMs. These observations suggest that eukaryotes may bear a

*To whom correspondence should be addressed. Tel: +81 82 424 6528; Fax: +81 82 424 0759; Email: shimizu@hiroshima-u.ac.jp

general mechanism by which they can eliminate autonomously replicating extrachromosomal genetic material.

To further extend the understanding of this issue, it is necessary to determine how an extrachromosomal DNA molecule behaves when placed in the nucleus or cytoplasm and how it is eliminated. Surprisingly, our understanding of these basic events is rather limited, even though it is well known that during transfection with an engineered DNA molecule, only a tiny amount of the DNA added is responsible for the transient transformation of the cells, and that almost all transfected molecules are lost from the cells during the early stage of transfection by an unknown mechanism. In contrast, unlike the question of how extrachromosomal DNA is eliminated, the question of how foreign DNA reaches the nucleus has been frequently addressed. For example, it has been shown that plasmid DNA up to 14 kb can move from the cytoplasm to the nucleus in digitonin-permeabilized cells (21). Moreover, by using the *Xenopus laevis in vitro* nucleus reconstruction system, it was shown that the foreign DNA molecule appeared to pass through the nuclear pore by passive diffusion (22). The nuclear transport of the plasmid DNA could be enhanced by coupling the plasmid DNA to the viral nuclear targeting signal sequence [for a review see ref. (23)], or by condensing the plasmid into a small particle by using the covalent conjugate between the cationic peptide melittin and poly (ethylenimine) (24).

The cellular uptake of plasmid DNA has been examined previously by calcium phosphate co-precipitation (25) or lipofection (26). However, our unpublished results have revealed that such techniques, as well as electroporation, result in the sticking of a huge amount of DNA aggregates to the outside of the cell surface (Supplementary Figure S1). Therefore, the only method available to answer our basic questions regarding foreign DNA behavior and elimination is the direct microinjection of the DNA molecule into the cytoplasm or the nucleus. Only few papers have addressed the fate of such microinjected DNA. For example, Lechardeur *et al*. (27) and Pollard *et al*. (28) examined what happens to DNA microinjected into the cytoplasm by fluorescence *in situ* hybridization (FISH). These authors found that the DNA rapidly disappeared and they suggested that cytoplasmic nuclease might be involved. However, the cell fixation or the detection of the DNA molecule by FISH, which involves DNA denaturation, may result in the artificial relocation or loss of the foreign DNA from the cells. However, Lukacs *et al*. (29) and Mearini *et al*. (30) have examined the diffusion rate of microinjected DNA molecules by analyzing fluorescence recovery after photobleaching (FRAP). Lukacs *et al*. (29) reported that diffusion in the cytoplasm of FITC-labeled linear DNA was dependent on its size, whereas the DNAs of all sizes became immobile after spreading through the nucleus. Mearini *et al*. (30) also reported that supercoiled DNA labeled by rhodamine-conjugated protein nucleic acid (PNA) diffused in the nucleus and became immobile because it bound to the nuclear matrix. However, no paper to date has analyzed the chronological order of the events that result in the elimination of foreign DNA. Thus, our objective of tracking injected DNA in live cells is absolutely necessary for enhancing our understanding of what happens to foreign DNA within the cell.

A major obstacle to such work is how to detect the injected DNA in live cells. Classical fluorescence dyes are easily bleached in live cells and require the injection of a relatively large amount of DNA. Furthermore, the effect of labeling on the intracellular behavior of the DNA should be carefully controlled. In this report, to detect injected DNA in live cells, we mainly used two methods that were based on completely different rationales. The first is the direct labeling of the DNA molecule by Alexa fluorochrome, which emits strong fluorescence and is hard to bleach. Another method was to inject DNA bearing the lactose operator (LacO) repeat sequence into the nucleus of cells expressing the lactose repressor (LacR)–GFP fusion protein. Both methods were sensitive enough to permit our detection and tracking of minimal amounts of foreign DNA in live cells and were used to complement the results of each other. Furthermore, we confirmed the results from live cells by using additional two methods that employed cell fixation; i.e. FITC-labeled DNA and the detection of naked DNA by FISH.

MATERIALS AND METHODS

Cell culture

Mouse embryonic fibroblasts from p53 gene knockout mice (MEF $p53^{-/-}$) and wild-type mice ($p53^{+/+}$) were kind gifts from Dr Otsura Niwa at Kyoto University (Kyoto, Japan). A retroviral vector expressing the LacR–GFP fusion protein was a kind gift from Dr Teru Kanda at Hokkaido University [Sapporo, Japan (31)]. HeLa cells were infected with the virus and the cells expressing weak and uniform green fluorescence in the nuclei were cloned and denoted as HeLa LacR–GFP cells in this study. The MEF $p53^{-/-}$, $p53^{+/+}$ cells and HeLa LacR–GFP cells were cultured in DMEM (Nissui, Pharmaceutical Co., Tokyo) supplemented with 10% fetal calf serum (FCS) in an air—5% CO_2 atmosphere with constant humidity.

The human adenocarcinoma cell line SW13, which is devoid of both keratins and vimentin, was a kind gift from Dr Masaki Inagaki at Aichi Cancer Center Research Institute (Nagoya, Japan) and was grown as described (32).

To synchronize the MEF $p53^{-/-}$ cells at G_0 phase by serum starvation, the cells were plated in glass-bottom dishes (MatTek Co., Ashland, MA), cultured overnight, washed with phosphate-buffered saline (PBS), and then further cultured in DMEM containing only 0.1% FCS for 68–72 h. The cells arrested at G_0 phase were released in fresh medium containing 10% FCS for 0, 4 and 12 h. The synchronization was evaluated by pulse labeling with 10 μM BrdU for 30 min. The incorporated BrdU was detected by a method previously described by us (13).

Preparation of DNA and protein solutions for the microinjection

All Alexa fluorochrome-conjugated DNAs were prepared by using PCR. The pSFVdhfr plasmid DNA (10 986 bp) served as the PCR template. The precise map of this plasmid appears in our previous paper (5). The 2798 bp DNA fragment was amplified from base position 5870–8668, the 400 bp fragment was from base position 882–1282 and the 258 bp fragment was from base position 5911–6169. The primers used to amplify the 400 and 258 bp fragments contained the NotI recognition sequence at their 5′ ends. The sequences of these primers will

be provided upon request. The PCR products gave sharp bands of the expected size when analyzed by agarose gel electrophoresis. A small portion of these PCR products was re-amplified in the presence of 20 μM of either Alexa Fluor 594-dUTP (Invitrogen Co., CA) or Alexa Fluor 488-dUTP (Invitrogen) plus 200 μM of dATP, dGTP, dCTP and dTTP. The product of the second PCR was treated with phenol-chloroform, precipitated by ethanol, and dissolved in high-quality sterile water at a concentration of 100 ng/μl. The resulting Alexa 594-conjugated linear 258 bp ('Alexa 594-lin.258'), 'Alexa 488-lin.400' and 'Alexa 594-lin.2,798' were then used in this study.

Alexa fluorochrome-conjugated relaxed circular (rc) DNA was prepared by the self-ligation of the Alexa 594-lin.258 or Alexa 488-lin.400 molecule. Since the PCR primers used to prepare these molecules contained the NotI recognition sequence, we completely digested the Alexa-conjugated linear molecule by NotI and the product was purified by a 'Performa DTR Gel Filtration Cartridge' (Edge BioSystems, MD). The DNA was ligated overnight at 16°C by using 0.03 U/μl of T4 DNA ligase (Toyobo, Osaka) at a DNA concentration of 1 ng/μl. The product was composed mainly of circularized monomer but also contained a small fraction of linear monomer and multimer (Supplementary Figure S2). To remove these linear molecules, we digested the ligation product with ATP-dependent deoxyribonuclease (Toyobo). After the digestion, the DNA was purified by phenol/chloroform and ethanol precipitation and dissolved in high-quality sterile water at a concentration of 100 ng/μl. The resulting 'Alexa 594-rc(258)n' and 'Alexa 488-rc(400)n' DNAs were then used in this study.

For the preparation of Alexa 594-conjugated rc(3,018)n DNA that codes LacR-CFP protein, the pSV2ECFP-LacI plasmid DNA (5653 bp) (33) served as the PCR template. The plasmid was a kind gift from Drs Susan M. Janicki and David L. Spector. The PCR product (3018 bp) spans the entire region of SV2 promoter. ECFP-LacR coding and the SV40 polyA sequences. Both the preparation of Alexa 594-conjugated linear DNA and the circularization by self-ligation were performed as the same procedure as described above. For the experiment appearing in Figure 3L, Alexa 594-conjugated lin.3018 DNA was completely digested by RQ-1 DNase (Promega) in DMEM without serum. The digest was boiled for 10 min to inactivate the DNase and directly injected to the cells.

To prepare LacO DNA, we used the pSV2-dhfr 8.32 plasmid (15 080 bp) (34) that was a kind gift from Dr Andrew Belmont at Illinois University (Urbana, IL). The plasmid contains the LacO repeat, which is 10 080 bp in length. The supercoiled (sc) DNA of the plasmid was purified by using the Qiagen plasmid purification kit (Qiagen Inc., Valencia, CA) and denoted as 'LacO sc15,080' DNA in this study. The LacO sc15,080 DNA was also linearized by SalI digestion, purified by phenol-chloroform treatment and ethanol precipitation, and denoted as 'LacO lin.15 080' DNA. The 10 080 bp LacO repeat was composed of 32 copies of a 315 bp unit that could be excised by EcoRI digestion. Therefore, we isolated the 315 bp fragment and rcDNA was prepared by the self-ligation reaction, as described in the preparation of the Alexa-conjugated rcDNA. In this case, the circular dimer was the major product (Supplementary Figure S2). The product was denoted as 'LacO rc(315)n'. The LacO sc15,080, LacO lin.15 080 and LacO rc(315)n DNAs were dissolved in water at a concentration of 30 ng/μl.

FITC-labeled sc pUC119 DNA (3162 bp) was prepared by using the 'Label-It fluorescein nucleic acids labeling kit' (Mirus Co., WI) and the plasmid DNA was purified by using the Qiagen plasmid purification kit according to the manufacturer's recommended protocol. The FITC-labeled DNA showed a single band in agarose electrophoresis that had the same mobility as the original unlabeled scDNA. The labeled DNA was dissolved in water at a concentration of 100 ng/μl and denoted as 'FITC-sc3,162'. When this DNA was used for the microinjection, the cells were fixed with 1.75% paraformaldehyde in PBS for 10 min at room temperature, counterstained with 4′,6-diamidino-2-phenylindole (DAPI; Sigma) and observed in the presence of antifade solution ('Vectashield'; Vector Lab. Inc., CA).

In most experiments, Alexa Fluor 594- or Alexa Fluor 488-conjugated DNA was mixed and co-injected with Alexa Fluor 488 goat anti-mouse IgG $F(ab')_2$ (Invitrogen Co., CA) or Alexa Fluor 594 rabbit anti-mouse IgG $F(ab')_2$ (Invitrogen), respectively. IgG protein was selected as it might not disturb the cellular functions. To remove the sodium azide that is included in the commercially available solutions as a preservative, we completely exchanged the buffer with PBS by using the 'Microcon' centrifugal filter device (YM-30, 30 000 MWCO; Millipore, MA). The concentration of the final solution was 4 μg/μl.

Microinjection and image acquisition

The cells were plated in glass-bottom dishes (No. 0, MatTek Co. Ashland, MA) the day before injection. To identify the injected cells, the cells were grown on 'CELLocate' coverslips (Eppendorf, Hamburg, Germany) placed on the glass-bottom dish, or grown directly on the glass-bottom dish sealed with a small piece of adhesive sealing film with a grid (Asahi Techno Glass Co., Tokyo). A few hours before injection, the cells were washed once with PBS and RPMI 1640 medium without phenol red (Sigma, St Louis, MO) containing 10% FCS was added. RPMI 1640 was used because its concentration of riboflavin, which emits weak fluorescence at a similar wavelength as Alexa 488, was half that of DMEM.

Just prior to injection, equal volumes of a 100 ng/μl DNA solution, a 4 μg/μl protein solution, and a 3× concentration of DMEM were mixed. The mixture (3–5 μl) was passed through a 'Millex-GV' 0.22 μm PVDF filter unit (Millipore, MA) by centrifugation at 6600 *g* for 2 min.

The cells on the dish were then placed on a thermoplate (Tokai Hit Co., Shizuoka, Japan) warmed to 37°C that had been placed on an inverted fluorescence microscope (ECLIPSE TE2000-U; Nikon). Microinjection was performed by using a micromanipulator (InjectMan; Eppendorf) working with a pump (FemtoJet; Eppendorf), with which the microscope was equipped. The injection sample was loaded into a 'FemtoTip' needle (Eppendorf) by using a microloader (Eppendorf). For the injection, an injection pressure of 30 hPa, a maintenance pressure of 5 hPa, and an injection time of 0.3–0.8 s were usually used. These constitute the empirically determined minimum required conditions, where the faint movement of the fluid in the cytoplasm or the nucleus

was visible without swelling of the cell structure under the phase contrast view using the ×40 objective. Zhang *et al*. (35) estimated the injection volume as 20 fl by using radioactive material and the same injection equipment under the quite similar condition. Employing the value, a single injection of 30 ng/μl corresponds roughly to 1700 molecule of 400 bp DNA. Short-term tracking (within 30 min) of the injected molecule was performed on the thermoplate. For longer term tracking, we incubated the cells in a CO_2 incubator. Images were obtained by using a ×40 objective (Nikon Plan Fluor, NA 0.60), the appropriate filter set specific for each fluorochrome, and a Fuji FinePix S1Pro digital camera (Fuji Film Co., Tokyo) at a setting of ISO 1600, 6 million pixels. The acquired digital images were merged by using Adobe Photoshop (R) version 4.0J.

RESULTS

Behavior and elimination of DNA injected into the cytoplasm

We at first examined the behavior of foreign DNA injected into the cytoplasm. Representative images are shown in Figure 1. Examination of >50 injected cells for each case

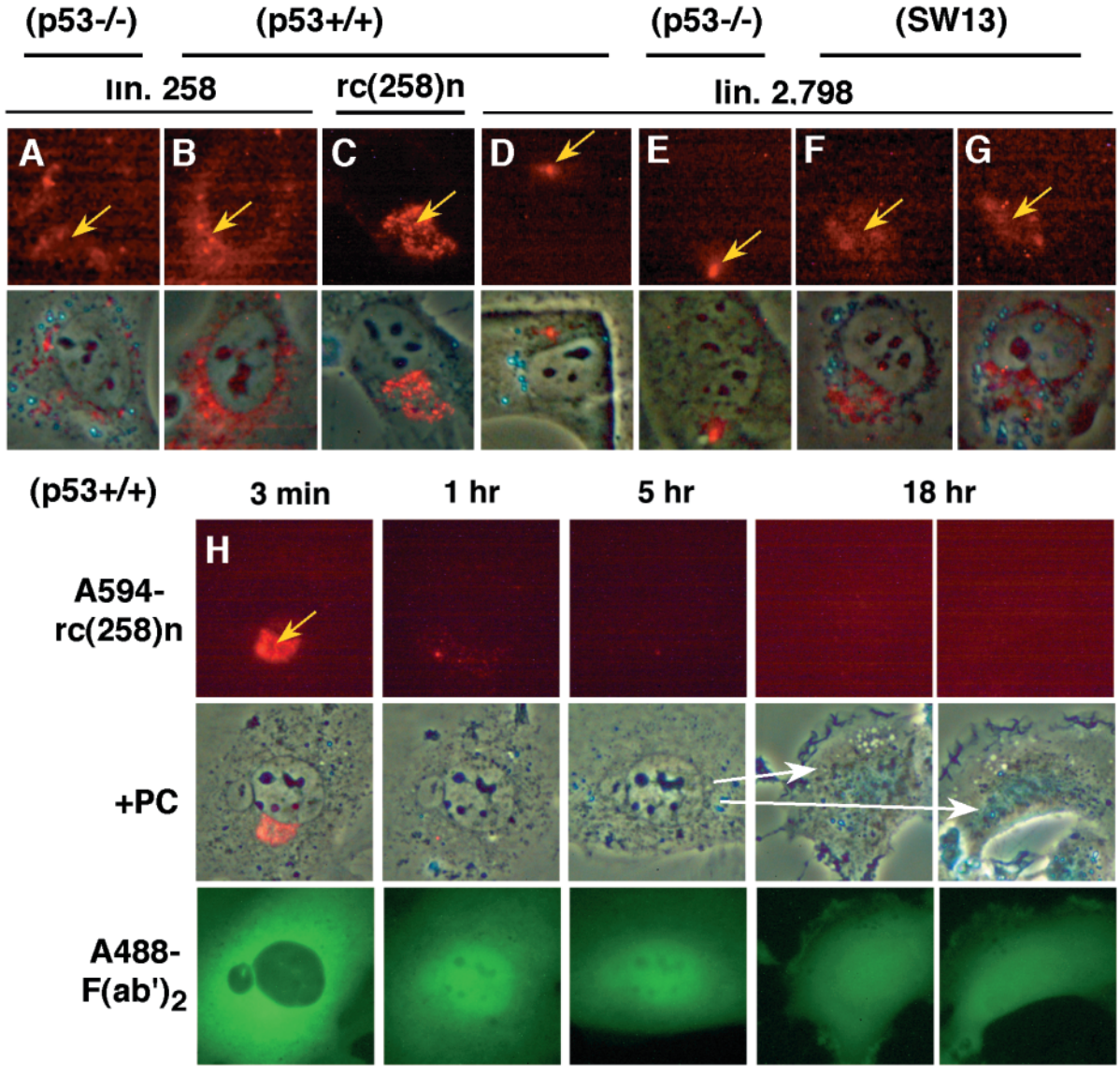

Figure 1. Intracytoplasmic diffusion and elimination of DNA injected into the cytoplasm. Alexa 594-labeled lin.258 (**A** and **B**), rc(258)n (**C** and **H**) or lin.2798 (**D**–**G**) was injected into the cytoplasm of MEF $p53^{-/-}$ (A and E), $p53^{+/+}$ (B–D and H), or SW13 (**F, G**) cells. After 3 min of injection [except for (H)], or at the times indicated in the images [for (H)], both the fluorescence DNA images and the phase contrast images (PC) were taken. The former images (upper images), and these images merged with the latter images (lower images), are shown. In (H), Alexa 488-conjugated IgG $F(ab')_2$ protein was co-injected with DNA and its fluorescence images at each time point are also shown. The yellow arrows indicate the injection sites. Relatively short linear DNA diffused widely with slight aggregation throughout the cytoplasm of the MEF cells at 3 min (A and B) whereas longer DNA did not (D and E). The diffusion of circular DNA [(C and H); 3 min] was more restricted than the linear DNA of similar size (A and B). The diffusion of the longer DNA may be inhibited by the cytoplasmic intermediate filament since the longer DNA did diffuse widely throughout the cytoplasm of the SW13 cells (F and G). The DNA injected into the cytoplasm disappeared rapidly whereas the co-injected protein was retained for a much longer period (H). The white arrows in (H) show the cell division between 5 and 18 h.

revealed that Alexa 594-labeled linear 258 bp (lin.258) DNA always diffused widely throughout the cytoplasm within 3 min, whereas the rc 258 bp ladder rc(258)n always diffused less than the linear DNA and was much more aggregated (Figure 1A–C and H). This was true for both the MEF $p53^{+/+}$ and $p53^{-/-}$ cells. In contrast, relatively long Alexa 594-labeled linear 2798 bp DNA (lin.2798) did not diffuse throughout the cytoplasm of either MEF $p53^{+/+}$ or $p53^{-/-}$ cells; rather, it was always (after injection to 35 or 42 cells, respectively) retained at the injection site (Figure 1D and E) 3 min after the injection. Therefore, the diffusion of the foreign DNA throughout the cytoplasm upon microinjection is clearly dependent on both the linearity and the size of the DNA injected. However, if Alexa 594-labeled lin.2798 DNA was injected into the cytoplasm of SW13 cells that lack cytoplasmic keratin and vimentin, it always (after injection to 35 cells) diffused quite differently to that in MEF cells, as the DNA diffused throughout a relatively wide area, despite the length of the DNA (Figure 1F and G).

We next chased the injected DNA over a prolonged period after injecting a mixture of Alexa 594-labeled rc(258)n DNA and Alexa 488-labeled protein into the cytoplasm of MEF $p53^{+/+}$ cells. Representative images from such experiments appear in Figure 1H. The DNA moderately diffused with weak aggregation within 3 min after the injection, as seen in above, and disappeared rapidly after that since the DNA was barely detectable at 1 h and was undetectable at 5 or 18 h. In contrast, the co-injected protein was stable as almost the same amounts as those that were injected were detected, even after cell division. Since the injected IgG $F(ab')_2$ protein did not show a sub-cellular localization signal, it diffused through the cytoplasm to the nucleus and at 1 h after the injection was almost evenly distributed throughout the cell. As the Alexa 488 fluorochrome that was used to label the protein is excited by a shorter wavelength light, it bleaches faster than the Alexa 594 fluorochrome that was used to label the DNA (F. Kamezaki, unpublished data). Therefore, the rapid disappearance of Alexa 594-labeled DNA that we observed is not owing to the bleaching. Furthermore, we performed five independent time-lapse experiments and quantify the cell-associated fluorescent signal. The result summarized in Figure 2A suggested that the DNA injected at the cytoplasm disappeared rapidly within 5 h.

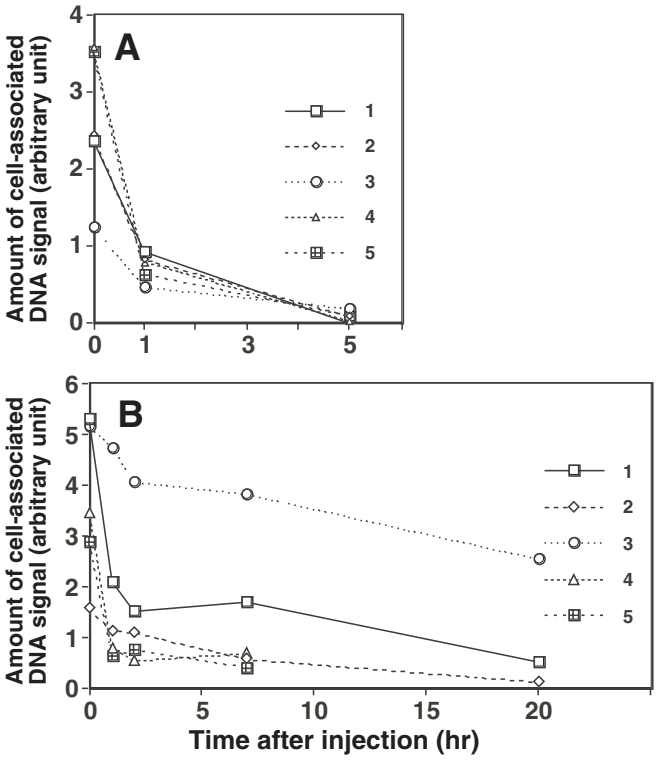

Figure 2. Decrease in the overall level of DNA in a cell after the injection into the cytoplasm or the nucleus. Alexa 594-labeled rc(258)n was injected into the cytoplasm (**A**) or the nucleus (**B**) of MEF $p53^{-/-}$ cells. After the incubation for the indicated time, photographs of the fluorescence images were taken with the identical condition. From such photographs, the amount of cell-associated fluorescence was measured by using NIH image 1.62. Background fluorescence, which was measured in the same area at the neighboring field of the target cell, was subtracted for each image.

Behavior of DNA injected into the nucleus

We microinjected Alexa 594-labeled lin.2798 DNA into the nucleus of MEF $p53^{+/+}$ (Figure 3A), MEF $p53^{-/-}$ (Figure 3B), and HeLa cells (Figure 3C). Examination of >30 injected cells for each case revealed that the longer DNA always diffused poorly in the nucleus and appeared as an aggregate at the site of injection. When LacO repeat DNA was microinjected into the nucleus of HeLa LacR–GFP cells, the injected DNA was visualized within 1–3 min. This was because the LacR-GFP protein, which had been diffusely distributed in the nucleus, rapidly bound to the LacO repeat sequences (36), and because the large protein molecule could diffuse freely in the nucleus even in the condensed chromatin (37). If 15 080 bp supercoiled plasmid DNA containing the 10 kb LacO repeat (LacO sc15,080; Figure 3D) or its linearized molecule (LacO lin.15 080; Figure 3E) was injected, the visualized DNA always (42/42 or 40/40 injected cells, respectively) appeared as an aggregate at the site of injection. In Figure 3E the nucleus is not full of GFP and only the DNA remains visible, whereas in Figure 3D both the nucleus and the DNA features GFP. This was because the level of LacR-GFP protein varied slightly between the cells even among the clonal cell population. Therefore, we concluded that longer DNA could not diffuse throughout the nucleus of the cells examined, regardless of whether it is linear or supercoiled.

In contrast, if shorter DNA was injected, it diffused rapidly throughout the nucleus (Figure 3F–S). This was always (>30 injected cells for each combination of DNA and cell) demonstrated by using Alexa 488-labeled DNA, Alexa 594-labeled DNA and LacO DNA. This high diffusibility was not affected by either the linearity or circularity of the DNA or whether the p53-mediated checkpoint machinery was present. In all cases examined with no exception, the injected DNA rapidly diffused within 1 min and formed small aggregated particles. Time-lapse observations revealed that the DNA was not aggregated at the time of injection and became aggregated rapidly in a order of few tens of seconds in the nuclear environment (Figure 3K). In contrast, if the DNase digest of Alexa 594-labeled DNA was injected, it was not aggregated and dispersed throughout the nucleus within 3 min (Figure 3L), and rapidly leaked to the cytoplasm. Furthermore, if the various concentration of Alexa 594-labeled rc(3,018)n DNA that

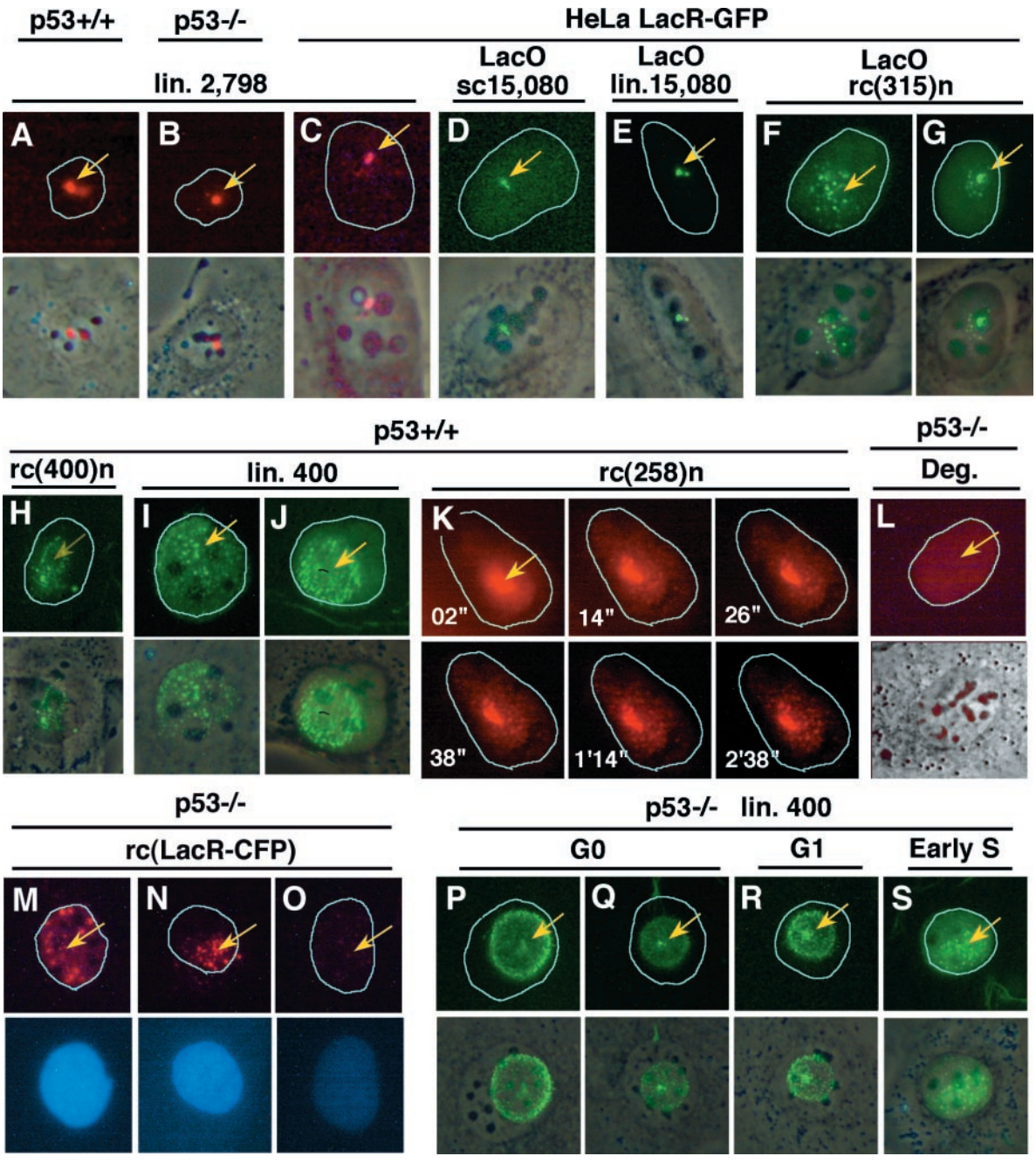

Figure 3. Intranuclear diffusion and aggregation of foreign DNA shortly after its injection into the nucleus. Alexa 594-labeled lin.2,798 (**A**–**C**), rc(258)n (**K**), rc(3,018)n DNA that expresses LacR-CFP (**M**–**O**), its DNase digest (**L**), Alexa 488-labeled rc(400)n (**H**), lin.400 (**I**, **J** and **P**–**S**), LacO sc15,080 (**D**), LacO lin.15,080 (**E**) or LacO rc(315)n (**F** and **G**) was injected into the nucleus of MEF $p53^{+/+}$ (A and H–K), MEF $p53^{-/-}$ (B and L–S), or HeLa LacR-GFP (D–G) cells. The effect of cell cycle stage on foreign DNA distribution was examined by synchronizing MEF $p53^{-/-}$ cells by serum starvation (P–S). DNA solution (100 ng/μl) was used for the injection, except (M) 300 ng/μl, (N) 100 ng/μl and (O) 30 ng/μl. After 3 min of the injection [except (K and M–N)], at the times indicated in the images [for (K)], or 3 h after the injection (M–O), both the fluorescence DNA images and the phase contrast images were taken. The former images (upper images), and these images merged with the latter (lower images), are shown except for (K and M–O). The lower panels of (M–O) show the cyan fluorescence emitted from LacR-CFP. In all the fluorescence images, the nucleus rim was outlined with cyan lines. The yellow arrows indicate the injection sites. The longer DNA did not diffuse throughout the nucleus regardless of whether it was linear (A–C and E) or super-coiled (D). In contrast, the shorter DNA diffused widely and aggregated. The aggregation occurred in a few tens of seconds (K). The DNase digest was not aggregated (L). Gene expression occurred from the aggregated DNA in DNA dose-dependent manner (M–O). In some cells, the aggregate formed a ring (G, H, J, K and P–R) in the nucleus. Such a ring-shaped arrangement was obvious in the G_0 (P and Q) and the G_1 cells (R) but not in the early S phase cells (S).

codes LacR-CFP protein was injected into the nucleus, the DNA was similarly aggregated at any DNA concentration. In these cells, LacR-CFP protein was expressed almost proportional to the amount of DNA injected. (Figure 3M–O), suggesting that the gene expression occurred from the aggregated DNA.

Notably, in a portion of the injected cells, the aggregates were arranged inside the nucleus as rings with varying radii

(Figure 3G–H, J and P–R). Among these cells, the aggregate was also visible at the center of ring that corresponded to the injection site (Figure 3P–R). Despite the fact that the cells obtained from a logarithmically growing culture were injected in an identical fashion, rings were not observed in all cells. This may reflect differences in the physiological condition of the cells, most probably the cell cycle stage. To test this, we arrested MEF p53$^{-/-}$ cells by serum starvation (the G_0 population) and then released the cells by cultivation in medium containing 10% FCS for 4 h (the G_1 population) or 12 h (the early S population). BrdU-pulse labeling and the detection of incorporated BrdU revealed that of the G_0 and the G_1 populations, 10.3 and 14.0% of the cells still underwent DNA replication, respectively. In contrast, 74.7% of the early S population showed BrdU-labeling whose intranuclear pattern was typical of the early S phase (13). We then simultaneously injected these three populations with Alexa 488-lin. 400 DNA using the same conditions. We found that 17 of 20 G_0 cells (Figure 3P–Q), 16 of 20 G_1 cells (Figure 3R), and 2 of 20 early S cells (Figure 3S) showed the typical ring-shaped arrangement of the aggregates. These fractions are very close to the fractions that did not show BrdU-incorporation. Thus, it appears that the ring-shaped arrangement of the aggregates preferentially formed if the cells were at the G_0/G_1 phase.

Movement of injected DNA from the nucleus to the cytoplasm, followed by its elimination

We then chased the intranuclear-injected DNA over a longer period. Unexpectedly, when we injected MEF p53$^{-/-}$ cells with a mixture of Alexa 488-lin.400 DNA and Alexa 594-labled protein, a portion of the DNA appeared in the cytoplasm within 1 min (Figures 4A and 5A) and localized at the rim. This was qualitatively reproducible in >70 cells among 100 injected cells, regardless with Alexa488- or Alexa 594-labeling. Since a small portion of the co-injected protein also appeared in the cytoplasm (Figure 4A, lower panel), it was possible that some of the injected solution had leaked into the cytoplasm at the time of injection. However, Figure 1H

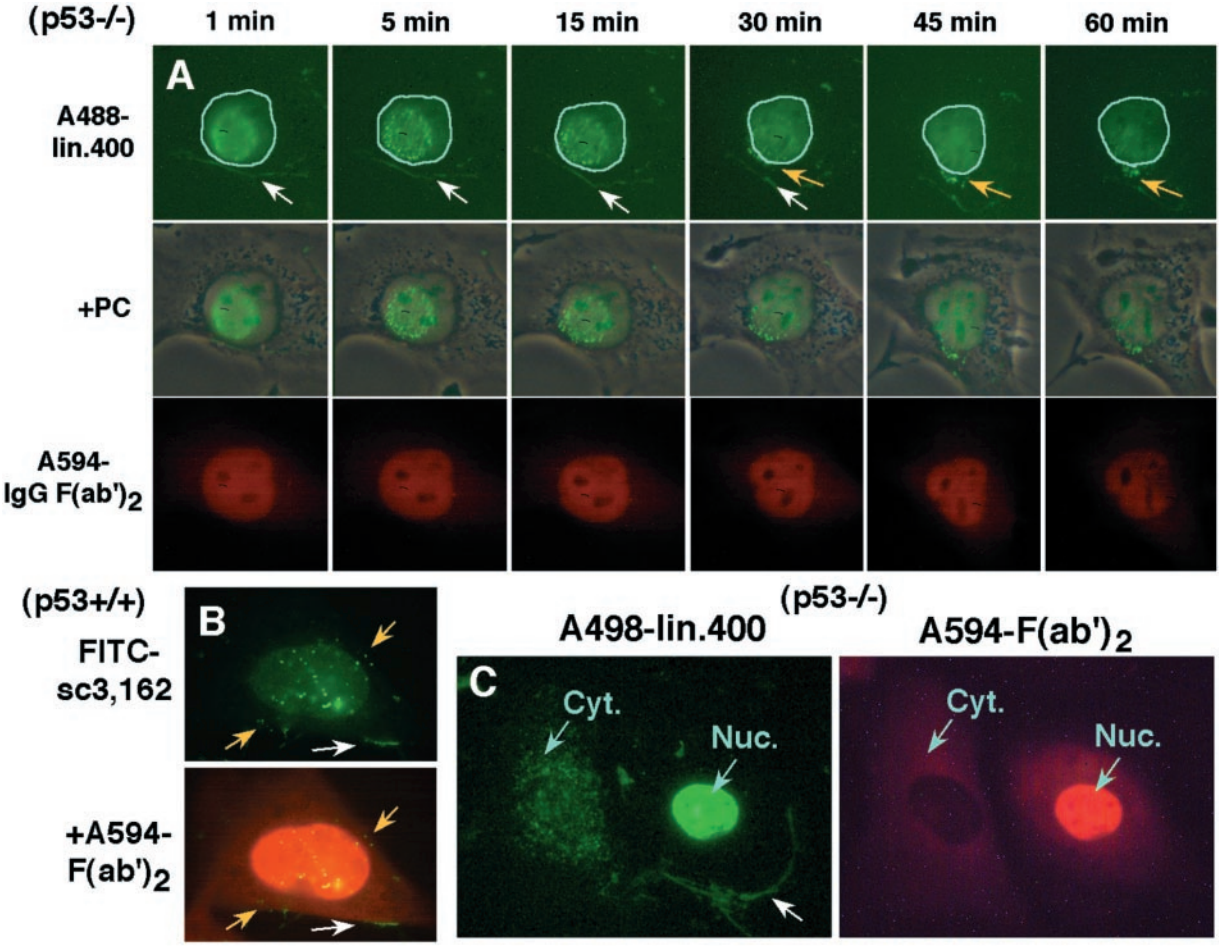

Figure 4. Movement to the cytoplasm of DNA injected into the nucleus. (**A**) Alexa 488-labeled lin. 400 DNA was mixed with Alexa 594-labeled IgG F(ab′)$_2$ protein, and co-injected into the nucleus of MEF p53$^{-/-}$ cells. Within 1 min, the injected DNA appeared at the periphery of the cytoplasm (white arrows). Furthermore, a portion of the aggregates that were formed within the nucleus moved to the cytoplasm: this was obvious at 30, 45 and 60 min (yellow arrows). In the fluorescence images, the nucleus rim was outlined with cyan lines. (**B**) FITC-labeled sc3,162 DNA was injected into the nucleus of MEF p53$^{+/+}$ cells and the cells were fixed 30 min later. A portion of the DNA was detected at either the cytoplasmic rim (white arrow) or as an aggregate in the cytoplasm (yellow arrow). (**C**) The cells were injected as described in (A). If the DNA was injected into the nucleus (Nuc.), a portion of it was detected at the cytoplasmic rim at 3 min after the injection (white arrow), whereas direct injection into the cytoplasm (Cyt.) did not lead to this distribution.

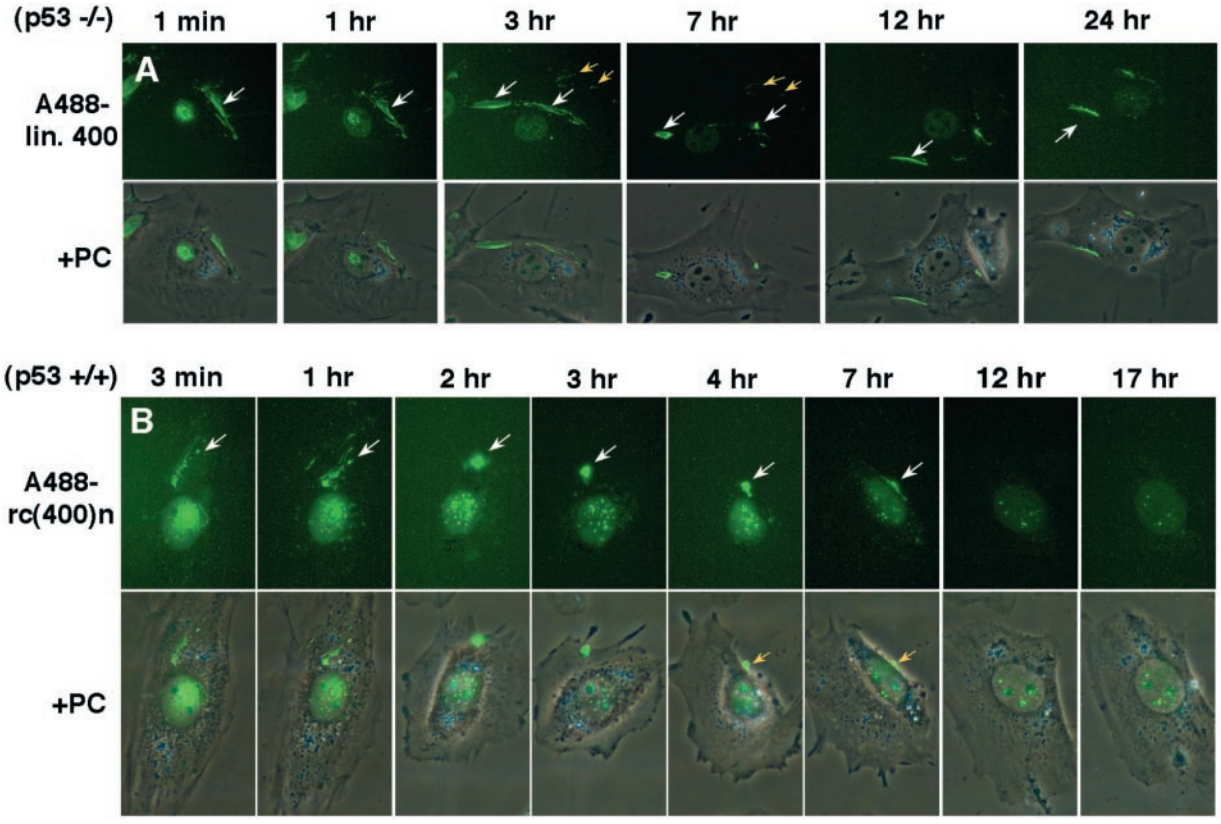

Figure 5. Elimination of the DNA injected into the nucleus. Alexa 488-labeled lin. 400 (**A**) or rc(400)n DNA (**B**) was injected into the nucleus of MEF $p53^{-/-}$ (A) or $p53^{+/+}$ cells (B). Fluorescence images (upper images) and the same images merged with the phase contrast images (lower images) obtained at different times after injection are shown. In the nucleus, the injected DNA appeared initially as a ring [(A); 1 min) and became aggregated (A and B). The amount of injected DNA left in the nucleus decreased as time progressed (A and B). Very early after injection [1 min in (A) and 3 min in (B)], a portion of the injected DNA appeared at the rim of the cytoplasm, as shown in Figure 4. Such DNA moved actively from one side of the cell to the other [white arrow in (A); see 3–12 h) and occasionally disappeared [white arrow in (B); from 7 to 14 h). A portion of the injected DNA appeared outside the cells [yellow arrows in (A); see 3 and 7 h].

suggests that the protein may actually move across the nuclear membrane. Furthermore, the DNA that appeared in the cytoplasm after the intranuclear injection differed in its distribution to the DNA that was injected directly into the cytoplasm: the former localized at the cytoplasmic rim (Figure 4C, right panel) while the latter localized diffusely throughout the cytoplasm (Figure 4C, left panel). The peri-cytoplasmic distribution of the intranuclear-injected DNA was also evident when FITC-labeled sc (sc3,162) DNA (Figure 4B) or Alexa 488-labeled rc [rc(400)n] DNA (Figure 5B) was injected into the nucleus. In the case of the mixture of Alexa 488-lin.400 DNA and Alexa 594-labeled protein (Figure 4A), the injected DNA formed a ring-shaped arrangement in the nucleus by 1 min and aggregated into small particles by 5 min, as described above. Surprisingly, the aggregates also gradually passed through the nuclear rim in the 15–30 min after the injection. These aggregates were clearly in the cytoplasm 45 and 60 min after the injection. This was qualitatively reproducible among three independent time-lapse experiments. Furthermore, we injected FITC-labeled sc3,162 DNA to the nucleus of MEF $p53^{+/+}$ cells, chased for a different time, fixed and scored the frequency of the intracellular localization of FITC signal (Table 1). The result showed that the fluorescent signal gradually moved to the cytoplasm. Taken together, the DNA injected into the nucleus is able to move to the cytoplasm.

The DNA that localized at the cytoplasmic rim appeared to be highly mobile. An example can be seen in Figure 5A. This figure shows that the Alexa 488-labeled lin. 400 DNA that was injected into the nucleus moved to the rim within 1 min and retained there until 3 h, then moved through the cytoplasm (7 h) to another side of the rim (12 h), where it was maintained for up to 24 h. However, in some cases, such DNA suddenly disappeared from the cells. As shown in Figure 5B, a portion of the intranuclear-injected Alexa 488-labeled rc(400)n DNA appeared as a large aggregate at the cytoplasmic rim, persisted there during 2–7 h, and then disappeared after 12 h. In most time-lapse experiments (>15 times), the amount of injected DNA that remained in the nucleus decreased markedly until 10–15 h after injection (Figure 5A and B and Supplementary Figure S3A) in a way that could not be explained by photobleaching.

There was also a significant amount of DNA that was retained in the nucleus for a longer period. Representative examples for Alexa 594 labeled rc(258)n DNA injected into MEF $p53^{+/+}$ cells (Figure 6A) or LacO rc(315)n DNA injected into HeLa LacR-GFP cells (Figure 6B) are shown. In both cases, the aggregated DNA remained in the nucleus until the cells entered mitosis, after which the DNA was left in the cytoplasm in all cases examined. This was qualitatively reproducible among 15 independent time-lapse experiments.

Table 1. Sequential change in the localization of fluorescent DNA signal

Location of the signal	Time after the injection				
	40 min	1.5 h	6 h	12 h	24 h
>80% at nucleus	79 (124/158)	43 (66/154)	39 (56/144)	22 (30/134)	4 (8/131)
Nucleus and cytoplasm	18 (29/158)	47 (72/154)	28 (40/144)	15 (20/134)	6 (12/181)
>80% at cytoplasm	3 (5/158)	10 (16/154)	31 (44/144)	58 (78/134)	77 (137/181)
None	0 (0/158)	0 (0/154)	2.8 (4/144)	4.5 (6/134)	13 (24/181)

FITC-sc3,162 DNA was mixed with Alexa 594-conjugated IgG F(ab′)2, and the mixture was injected to the nucleus of MEF $p53^{+/+}$ cells. After incubating for the times indicated, the cells were fixed with PFA and examined under fluorescence microscopy. The localization of FITC-fluorescence at either the nucleus or the cytoplasm was recorded among the cells with Alexa 594-fluorescence. In the table, the percentages of cells exhibiting either FITC-localization were shown, together with the actual number of cells (parenthesized).

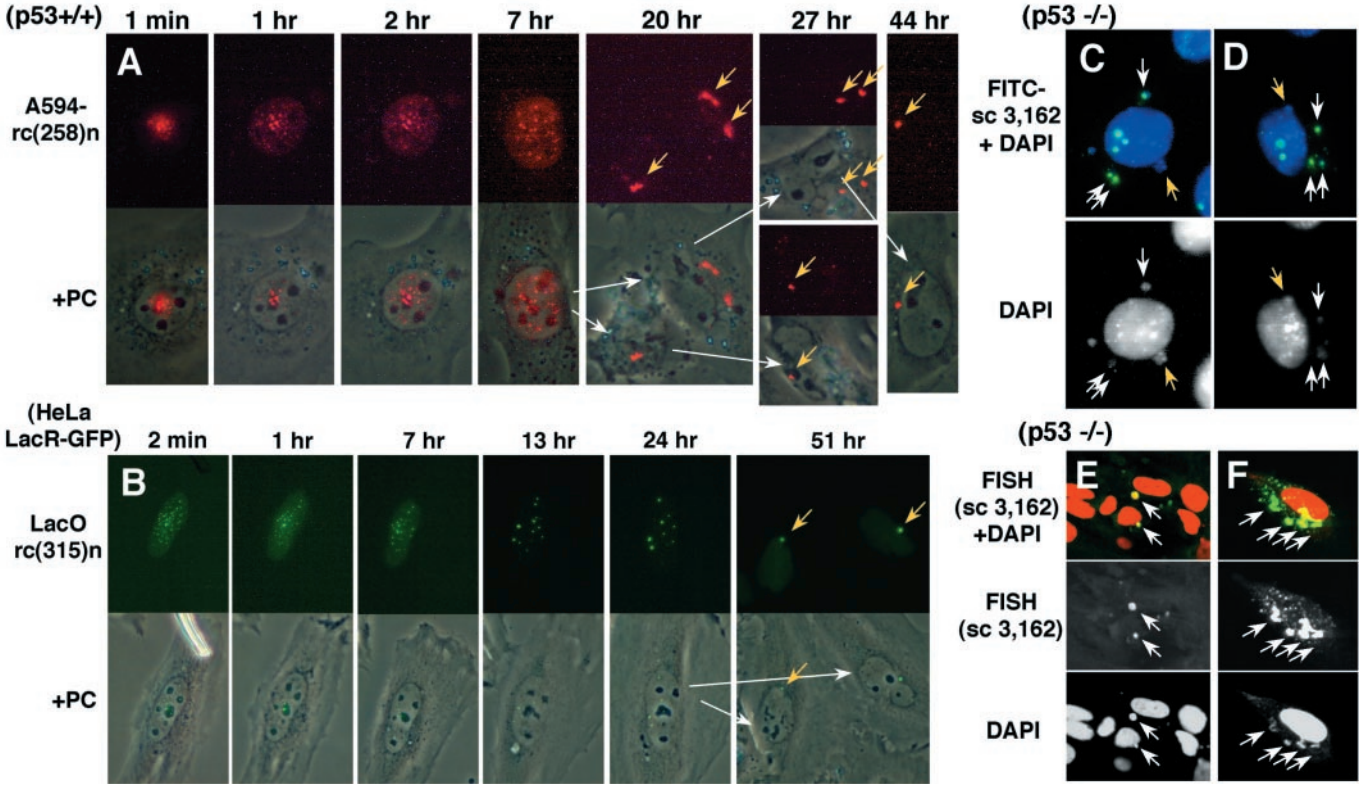

Figure 6. Stabilization of intranuclear-injected DNA in the nucleus and its localization in the cytoplasm after mitosis. Alexa 594-labeled rc(258)n (**A**) or LacO rc(315)n DNA (**B**) was injected into the nucleus of MEF $p53^{-/-}$(A) or HeLa LacR-GFP (B) cells. The injected DNA aggregated in the nucleus (A and B) and the number of aggregates decreased as time progressed (B). After mitosis, the aggregated DNA appeared in the cytoplasm near the nucleus [(A and B); yellow arrows). Such cytoplasmic aggregates were also detected where FITC-labeled sc 3,162 DNA was injected into the nucleus of MEF $p53^{-/-}$ cells and fixed with paraformaldehyde at 24 h (**C, D**). Furthermore, unlabeled sc 3,162 (pUC119) DNA was injected into the nucleus of MEF $p53^{-/-}$ cells and fixed with paraformaldehyde at 24 h (E and F). The injected DNA was detected by FISH using a probe prepared from pUC119 DNA. The cellular DNA was counter-stained with DAPI (C and D) or propidium iodide (**E** and **F**). In this case as well, the DNA was detected as aggregates in the cytoplasm. In (C–F), higher concentrations of DNA [200 ng/μl in (C and D), and 500 ng/μl in (E and F)] were injected compared with the normal conditions employed in this study. In these cases, the cytoplasmic aggregate (white arrows) looked just like micronucleus that was spontaneously formed in these cells (yellow arrows).

Furthermore, we also observed the aggregated DNA in the cytoplasm when we injected FITC-labeled scDNA into the nucleus and fixed the cells 24 h later (Figure 6C and D), or when we injected unlabeled scDNA into the nucleus, fixed the cells 24 h later and detected the injected DNA by FISH (Figure 6E and F). In Figure 6C–F, we injected much higher concentrations of DNA than before; the cytoplasmic aggregates that appeared resembled micronuclei.

Furthermore, we performed five additional and independent time-lapse experiments using Alexa 594-labeled DNA and quantified the overall level of DNA in a cell during the time course. The result summarized in Figure 2B suggested that the decrease in the fluorescence signal after the nuclear injection was biphasic. Namely, the signal rapidly decreased during initial few hours, then slowly decreased during longer hours.

Effect of the p53-mediated checkpoint pathway

To determine whether the p53-mediated checkpoint pathway can influence the behavior and elimination of the injected DNA, we compared MEF $p53^{-/-}$ cells and the $p53^{+/+}$ cells. Furthermore, we compared circular and linear DNAs whose

Table 2. Frequency of apoptotic cells among injected cells

Cell	Injection	Time (h)	TUNEL-positive cells (%)		
			IgG	scDNA	linear DNA
MEF $p53^{+/+}$	Nucleus	0.5	0	0	
		6	0	12.5	61.5
	Cytoplasm	0.5	0	0	0
		6	0	0	95
MEF $p53^{-/-}$	Nucleus	0.5	0	0	0
		6	0	0	0
	Cytoplasm	0.5	0	0	0
		6	0	8.5	0

Either the FITC-labeled sc or linear pUC118 DNA, or the FITC-conjugated IgG (Goat anti-mouse Ig; ICN pharmaceuticals, Irvine, CA) was independently injected at the nucleus or the cytoplasm of either MEF $p53^{+/+}$ or $p53^{-/-}$ cells. For each injection, duplicate of at least 50 cells were injected, incubated and fixed at 0.5 and 6 h. The apoptotic cells were detected by the TUNEL methods (12). The fraction of the number of cells with both FITC- and TUNEL-signal divided by the number of initially injected cells was shown.

only difference was the presence of a double-strand end. The linear DNA efficiently induced p53-dependent apoptosis when it was injected into either the nucleus or the cytoplasm (Table 2). This is consistent with a previous report showing that intranuclear-injected DNA can activate the p53-mediated checkpoint machinery (38). Our result suggested that the aggregated DNA at the nucleus could trigger the apoptotic signal. Furthermore, we found that the cytoplasmic DNA could also trigger apoptosis via the p53 pathway, probably because it moved to the nucleus, where it triggered the p53 damage response pathway. However, in none of the experiments described above could we detect any differences with respect to the behavior or elimination of injected DNA between $p53^{+/+}$ and $p53^{-/-}$ cells, or between linear and circular DNA.

DISCUSSION

In this paper, we have shown the dynamic behavior of the DNA molecule after it is placed into the cytoplasm or the nucleus. Our understanding of these dynamics (i.e. the chronological order of the events involved) requires chasing the DNA molecule over time in live cells, yet such analyses have not been reported to date.

In the cytoplasm, the diffusibility of the injected DNA molecule depended on its size. This observation is consistent with a previous report, where the diffusion of a cytoplasmically placed DNA was examined by FRAP (29). Furthermore, we have shown that the diffusibility was apparently different between linear and circular molecule. Since longer DNA diffused widely in the cytoplasm of SW13 cells, keratin or vimentin filament may normally block the diffusion of injected DNA in a DNA size-dependent manner. When short DNA was injected into the cytoplasm, it aggregated weakly and developed a particulate appearance, especially for circular molecule. This is consistent with images appearing in previous papers (27,29,30,39). By chasing the injected molecule, we showed that DNA injected into the cytoplasm disappeared rapidly. This confirmed previous reports, where the injected molecule was detected in fixed cells by FISH (27,28). These authors proposed that the cytosolic nuclease might be responsible for the degradation of the injected molecule.

Upon injection into the nucleus, the diffusion of the injected DNA was also size-dependent. This result was consistent with a previous report that employed FRAP analysis (29). After its diffusion, relatively short DNA rapidly aggregated in the nucleus. We could not completely rule out the possibility that the injected DNA might be physico-chemically precipitated in the nuclear environment. However, the DNA appeared to be transcribed (Figure 3M–O) or stimulated the apoptotic signal (Table 2) in its aggregated states. Therefore, its aggregation is most plausibly explained by its charge neutralization by the binding of some kind of basic molecule, since naked DNA has a negative charge in neutral pH. The binding between the DNA and this putative basic molecule must occur within a few tenths of a second, as was also seen for the binding of LacR-GFP protein to LacO repeat DNA. This was consistent with our observation that the aggregate of short DNA were initially arranged as a ring. The ring-shaped arrangement can be most plausibly explained by the aggregation of the DNA as it diffuses; the aggregation would lead to its loss of mobility and the sedimentation of the DNA in a ring shape. The aggregate might also be visible at the center of ring that corresponded to the injection site. It might be explained that the local concentration of the putative DNA-binding molecule might limit the diffusion. If this hypothesis is true, the appearance and radius of the ring may reflect the amount of the putative DNA-binding molecule that aggregates the foreign DNA. We have shown that the amount of molecule may be higher in G_0/G_1 cells and decreases after S phase.

Only few images showing the fate of intranuclear-injected DNA have been published. Pollard *et al*. (28) injected an unlabeled sc plasmid DNA into the nucleus of COS 7 cells and detected it by FISH after fixation. In those images, the DNA aggregated in the nucleus, which is consistent with our observations. In contrast, Mearini *et al*. (30) showed that the PNA-labeled sc plasmid DNA was distributed throughout the nucleoplasm without apparent aggregation. Since scDNA is compact in shape, it may diffuse freely. However, when we injected the sc FITC-labeled plasmid (Figure 4B) or the LacO plasmid (Figure 3D and E), the DNA did not diffuse and remained at the injection site. The disparity between our results and those of Mearini *et al*. (30) may be due to the fact that they used an almost 10-fold higher concentration of DNA (0.5–1 μg/μl) than we did (30–100 ng /μl). Alternatively, the difference may be due to the DNA-labeling methods or cells that were used.

We showed that the shorter DNA injected at the nucleus could transverse the nuclear membrane and appeared at the cytoplasmic rim within a few minutes. Furthermore, even the aggregates that formed in the nucleus could move to the cytoplasm during few tens of minutes. If a portion of the injected DNA may be degraded in the nucleus, the product may diffuse to the cytoplasm as seen in Figure 3L; however, the degradation product can neither be aggregated nor localized to the cytoplasmic rim. These findings were very surprising but reproducible among the different experiments using differently labeled DNAs and different cells. This may be the first time such movement of DNA from the nucleus to the cytoplasm over time has been observed. In the images appearing in the paper of Mearini *et al*. (30), a portion of the DNA injected into the nucleus was clearly in the cytoplasm in an aggregated form 18 h after the injection, before the division of

the cells. However, Mearini *et al*. (30) did not mention this observation in the text, probably because they did not chase the DNA molecule and thus overlooked the significance of their observation. As we have described in the Introduction, the movement of large plasmid DNA from the cytoplasm to the nucleus has been reported frequently. Since this movement is suggested to be due to passive diffusion, backward diffusion from the nucleus to the cytoplasm is possible. However, the movement of the aggregated DNA to the cytoplasm during interphase may not be explicable by this diffusion theory. Rather, it may indicate the presence of a transport system for aggregated extrachromosomal genetic materials. This notion may also pertain to our previous report (40), where it was suggested that the DM aggregates may appear in the cytoplasm during interphase, not after mitosis. Indeed, our unpublished images shown in Supplementary Figure S4, where DMs were detected by FISH, are highly similar to the images shown in Figure 4A. To date, extensive studies revealed the mechanism underlying the export from and import to the nucleus of protein or RNA [for reviews see refs. (41,42)]. A single type of channel, the nuclear pore complex, mediates all movement across the nuclear envelope. Passive transport of small molecule through nuclear pore is unrestricted, but efficient transport of macromolecule requires nuclear localization signal. It remains to be clarified whether DNA, especially its aggregated form, may pass through nuclear pore or whether there exist some kind of signal that dictate nucleocytoplasmic transport of DNA.

The DNAs at the cytoplasm were eventually lost from the cells, which might be explained by the dynamic movement of the cytoplasmic membrane at the periphery. Indeed, DNA indicated by the yellow arrows in Figure 5A at 3 and 7 h appeared on the outside of the cell: this may be the extruded DNA. However, it was usually quite difficult to locate the injected DNA in the extracellular space. It may be that the extruded DNA loses its adhesion to the substratum and becomes very hard to detect. The mechanism involved may be similar to that proposed for the extrusion of micronuclei from the cell, namely, by cytoplasmic membrane brebbing (12). We have shown here that the decrease in the total amount of the intranuclear-injected DNA was biphasic (Figure 2B). The first acute phase occurred within $\sim$2 h and might be mediated by the degradation. The second slow phase occurred as if it contained stochastic process and might correspond to the extrusion of aggregated DNA.

However, the remaining DNA was retained in the nucleus for a prolonged period. Such aggregated DNA appeared not to suffer extensive DNA degradation, because the TUNEL assay that detect apoptotic DNA fragmentation could not produce any signal there (S. Shigematsu, unpublished data). We have shown here that the aggregate of intranuclear-injected DNA was left in the cytoplasm after mitosis. This is the first time this has been shown directly by chasing the DNA molecule. The aggregate left at the cytoplasm appeared to resemble micronuclei, which suggests its similarity to the pseudo-nucleus formed by the purified DNA and the proteins present in X.*laevis* egg extract (43,44). As described in the Introduction, autonomously replicating extrachromosomal genetic material such as DMs segregate by sticking to the mitotic chromosome. Otherwise, they are left behind the chromosomes during anaphase and form micronuclei at the following interphase. Interestingly, DMs left behind at anaphase usually aggregated (14), which suggests a connection to our result shown here. Recently, we found that such aggregated-and-left-behind DMs suffered double-strand breakage (N. Shimizu and N. Misaka, manuscript submitted). This suggests that some mechanism exists that aggregates abnormal extrachromosomal genetic material in the nucleus, thereby extruding it from the nucleus after mitosis.

These observations together suggest eukaryotic cells have an elimination system for foreign DNA.

SUPPLEMENTARY DATA

Supplementary Data are available at NAR Online.

ACKNOWLEDGEMENTS

The authors thank Dr Otsura Niwa (Kyoto University, Kyoto, Japan), Dr Teru Kanda (Hokkaido University, Sapporo, Japan), Dr Masaki Inagaki (Aichi Cancer Center Research Institute, Nagoya, Japan), Dr Susan M. Janicki (Cold Spring Harbor Laboratory, NY), Dr David L. Spector (Cold Spring Harbor Laboratory, NY) and Dr Andrew Belmont (Illinois University, IL) for their kind gifts of cell lines or plasmids used in this study. We also thank Dr Geoffrey M. Wahl (The Salk Institute, CA). A discussion with him 10 years previously stimulated N.S. to pursue this experiment. This work was supported in part by a Grant-in-Aid for Scientific Research (B) (Grant no. 14340238) and a Grant-in-Aid for Exploratory Research (Grant no. 14658232) to N.S., both of which were from the Japan Society for the Promotion of Science. Funding to pay the Open Access publication charges for this article was provided by the Japan Society for Promotion of Sciences.

Conflict of interest statement. None declared.

REFERENCES

1. Gaubatz,J.W. (1990) Extrachromosomal circular DNAs and genomic sequence plasticity in eukaryotic cells. *Mutat. Res*., **237**, 271–292.
2. VonHoff,D.D. (1991) New mechanisms of gene amplification in drug resistance (the episome model). *Cancer Treat. Res*., **57**, 1–11.
3. Wahl,G.M. (1989) The importance of circular DNA in mammalian gene amplification. *Cancer Res*., **49**, 1333–1340.
4. Shimizu,N., Miura,Y., Sakamoto,Y. and Tsutsui,K. (2001) Plasmids with a mammalian replication origin and a matrix attachment region initiate the event similar to gene amplification. *Cancer Res*., **61**, 6987–6990.
5. Shimizu,N., Hashizume,T., Shingaki,K. and Kawamoto,J.K. (2003) Amplification of plasmids containing a mammalian replication initiation region is mediated by controllable conflict between replication and transcription. *Cancer Res*., **63**, 5281–5290.
6. Shimizu,N., Nakamura,H., Kadota,T., Kitajima,K., Oda,T., Hirano,T. and Utiyama,H. (1994) Loss of amplified c-myc genes in the spontaneously differentiated HL-60 cells. *Cancer Res*., **54**, 3561–3567.
7. Eckhardt,S.G., Dai,A., Davidson,K.K., Forseth,B.J., Wahl,G.M. and VonHoff,D.D. (1994) Induction of differentiation in HL60 cells by the reduction of extrachromosomally amplified c-myc. *Proc. Natl Acad. Sci. USA*, **91**, 6674–6678.
8. VonHoff,D.D., McGill,J.R., Forseth,B.J., Davidson,K.K., Bradley,T.P., Van Devanter,D.R. and Wahl,G.M. (1992) Elimination of extrachromosomally amplified MYC genes from human tumor cells reduces their tumorigenicity. *Proc. Natl Acad. Sci. USA*, **89**, 8165–8169.
9. Ambros,I.M., Rumpler,S., Luegmayr,A., Hattinger,C.M., Strehl,S., Kovar,H., Gadner,H. and Ambros,P.F. (1997) Neuroblastoma cells can

actively eliminate supernumerary *MYCN* gene copies by micronucleus formation - sign of tumour cell revertance? *Eur. J. Cancer*, **33**, 2043–2049.
10. Canute,G.W., Longo,S.L., Longo,J.A., Shetler,M.M., Coyle,T.E., Winfield,J.A. and Hahn,P.J. (1998) The hydroxyurea-induced loss of double-minute chromosomes containing amplified epidermal growth factor receptor genes reduces the tumorigenicity and growth of human glioblastoma multiforme. *Neurosurgery*, **42**, 609–616.
11. Shimizu,N., Kanda,T. and Wahl,G.M. (1996) Selective capture of acentric fragments by micronuclei provides a rapid method for purifying extrachromosomally amplified DNA. *Nature Genet.*, **12**, 65–71.
12. Shimizu,N., Shimura,T. and Tanaka,T. (2000) Selective elimination of acentric double minutes from cancer cells through the extrusion of micronuclei. *Mutat. Res.*, **448**, 81–90.
13. Itoh,N. and Shimizu,N. (1998) DNA replication-dependent intranuclear relocation of double minute chromatin. *J. Cell Sci.*, **111**, 3275–3285.
14. Tanaka,T. and Shimizu,N. (2000) Induced detachment of acentric chromatin from mitotic chromosomes leads to their cytoplasmic localization at G1 and the micronucleation by lamin reorganization at S phase. *J. Cell Sci.*, **113**, 697–707.
15. Kanda,T. and Wahl,G.M. (2000) The dynamics of acentric chromosomes in cancer cells revealed by GFP- based chromosome labeling strategies. *J. Cell. Biochem.*, **35**, 107–114.
16. Bode,J., Fetzer,C.P., Nehlsen,K., Scinteie,M., Hinrichs,B.-H., Baiker,A., Piechaczek,C., Benham,C. and Lipps,H.J. (2001) The hitchhiking principle: optimizing episomal vectors for the use in gene therapy and biotechnology. *Gene Ther. Mol. Biol.*, **6**, 33–46.
17. Marechal,V., Dehee,A., Chikhi-Brachet,R., Piolot,T., Coppey-Moisan,M. and Nicolas,J.C. (1999) Mapping EBNA-1 domains involved in binding to metaphase chromosomes. *J. Virol.*, **73**, 4385–4392.
18. Baiker,A., Maercker,C., Piechaczek,C., Schmidt,S.B., Bode,J., Benham,C. and Lipps,H.J. (2000) Mitotic stability of an episomal vector containing a human scaffold/matrix-attached region is provided by association with nuclear matrix. *Nature Cell Biol.*, **2**, 182–184.
19. Lehman,C.W. and Botchan,M.R. (1998) Segregation of viral plasmids depends on tethering to chromosomes and is regulated by phosphorylation. *Proc. Natl Acad. Sci. USA*, **95**, 4338–4343.
20. Ballestas,M.E., Chatis,P.A. and Kaye,K.M. (1999) Efficient persistence of extrachromosomal KSHV DNA mediated by latency-associated nuclear antigen. *Science*, **284**, 641–644.
21. Hagstrom,J.E., Ludtke,J.J., Bassik,M.C., Sebestyen,M.G., Adam,S.A. and Wolff,J.A. (1997) Nuclear import of DNA in digitonin-permeabilized cells. *J. Cell Sci.*, **110**, 2323–2331.
22. Salman,H., Zbaida,D., Rabin,Y., Chatenay,D. and Elbaum,M. (2001) Kinetics and mechanism of DNA uptake into the cell nucleus. *Proc. Natl Acad. Sci. USA*, **98**, 7247–7252.
23. Munkonge,F.M., Dean,D.A., Hillery,E., Griesenbach,U. and Alton,E.W. (2003) Emerging significance of plasmid DNA nuclear import in gene therapy. *Adv. Drug Deliv. Rev.*, **55**, 749–760.
24. Ogris,M., Carlisle,R.C., Bettinger,T. and Seymour,L.W. (2001) Melittin enables efficient vesicular escape and enhanced nuclear access of nonviral gene delivery vectors. *J. Biol. Chem.*, **276**, 47550–47555.
25. Batard,P., Jordan,M. and Wurm,F. (2001) Transfer of high copy number plasmid into mammalian cells by calcium phosphate transfection. *Gene*, **270**, 61–68.
26. Pastwa,E., Lubner,E.M., Mezhevaya,K., Neumann,R.D. and Winters,T.A. (2003) DNA uptake and repair enzyme access to transfected DNA is under reported by gene expression. *Biochem. Biophys. Res. Commun.*, **306**, 421–429.
27. Lechardeur,D., Sohn,K.J., Haardt,M., Joshi,P.B., Monck,M., Graham,R.W., Beatty,B., Squire,J., O'Brodovich,H. and Lukacs,G.L. (1999) Metabolic instability of plasmid DNA in the cytosol: a potential barrier to gene transfer. *Gene Ther.*, **6**, 482–497.
28. Pollard,H., Toumaniantz,G., Amos,J.L., Avet-Loiseau,H., Guihard,G., Behr,J.P. and Escande,D. (2001) Ca2+-sensitive cytosolic nucleases prevent efficient delivery to the nucleus of injected plasmids. *J. Gene Med.*, **3**, 153–164.
29. Lukacs,G.L., Haggie,P., Seksek,O., Lechardeur,D., Freedman,N. and Verkman,A.S. (2000) Size-dependent DNA mobility in cytoplasm and nucleus. *J. Biol. Chem.*, **275**, 1625–1629.
30. Mearini,G., Nielsen,P.E. and Fackelmayer,F.O. (2004) Localization and dynamics of small circular DNA in live mammalian nuclei. *Nucleic Acids Res.*, **32**, 2642–2651.
31. Kanda,T., Otter,M. and Wahl,G.M. (2001) Mitotic segregation of viral and cellular acentric extrachromosomal molecules by chromosome tethering. *J. Cell Sci.*, **114**, 49–58.
32. Inada,H., Izawa,I., Nishizawa,M., Fujita,E., Kiyono,T., Takahashi,T., Momoi,T. and Inagaki,M. (2001) Keratin attenuates tumor necrosis factor-induced cytotoxicity through association with TRADD. *J. Cell Biol.*, **155**, 415–426.
33. Janicki,S.M., Tsukamoto,T., Salghetti,S.E., Tansey,W.P., Sachidanandam,R., Prasanth,K.V., Ried,T., Shav-Tal,Y., Bertrand,E., Singer,R.H. *et al.* (2004) From silencing to gene expression: real-time analysis in single cells. *Cell*, **116**, 683–698.
34. Robinett,C.C., Straight,A., Li,G., Willhelm,C., Sudlow,G., Murray,A. and Belmont,A.S. (1996) *In vivo* localization of DNA sequences and visualization of large-scale chromatin organization using lac operator/repressor recognition. *J. Cell Biol.*, **135**, 1685–1700.
35. Zhang,J., Xu,F., Hashimshony,T., Keshet,I. and Cedar,H. (2002) Establishment of transcriptional competence in early and late S phase. *Nature*, **420**, 198–202.
36. Robinett,C.C., Straight,A., Li,G., Willhelm,C., Sudlow,G., Murray,A. and Belmont,A.S. (1996) *In vivo* localization of DNA sequences and visualization of large-scale chromatin organization using lac operator/repressor recognition. *J. Cell Biol.*, **135**, 1685–1700.
37. Verschure,P.J., van der Kraan,I., Manders,E.M., Hoogstraten,D., Houtsmuller,A.B. and van Driel,R. (2003) Condensed chromatin domains in the mammalian nucleus are accessible to large macromolecules. *EMBO Rep.*, **4**, 861–866.
38. Huang,L.-C., Clarkin,K.C. and Wahl,G.M. (1996) Sensitivity and selectivity of the DNA damage sensor responsible for activating p53-dependent G1 arrest. *Proc. Natl Acad. Sci. USA*, **93**, 4827–4832.
39. Ludtke,J.J., Sebestyen,M.G. and Wolff,J.A. (2002) The effect of cell division on the cellular dynamics of microinjected DNA and dextran. *Mol. Ther.*, **5**, 579–588.
40. Shimizu,N., Itoh,N., Utiyama,H. and Wahl,G.M. (1998) Selective entrapment of extrachromosomally amplified DNA by nuclear budding and micronucleation during S-phase. *J. Cell Biol.*, **140**, 1307–1320.
41. Quimby,B.B. and Corbett,A.H. (2001) Nuclear transport mechanisms. *Cell Mol. Life Sci.*, **58**, 1766–1773.
42. Weis,K. (2002) Nucleocytoplasmic transport: cargo trafficking across the border. *Curr. Opin. Cell Biol.*, **14**, 328–335.
43. Marini,N.J. and Benbow,R.M. (1991) Differential compartmentalization of plasmid DNA microinjected into *Xenopus laevis* embryos relates to replication efficiency. *Mol. Cell. Biol.*, **11**, 299–308.
44. Gilbert,D.M., Miyazawa,H. and DePamphilis,M.L. (1995) Site-specific initiation of DNA replication in Xenopus egg extract requires nuclear structure. *Mol. Cell. Biol.*, **15**, 2942–2954.

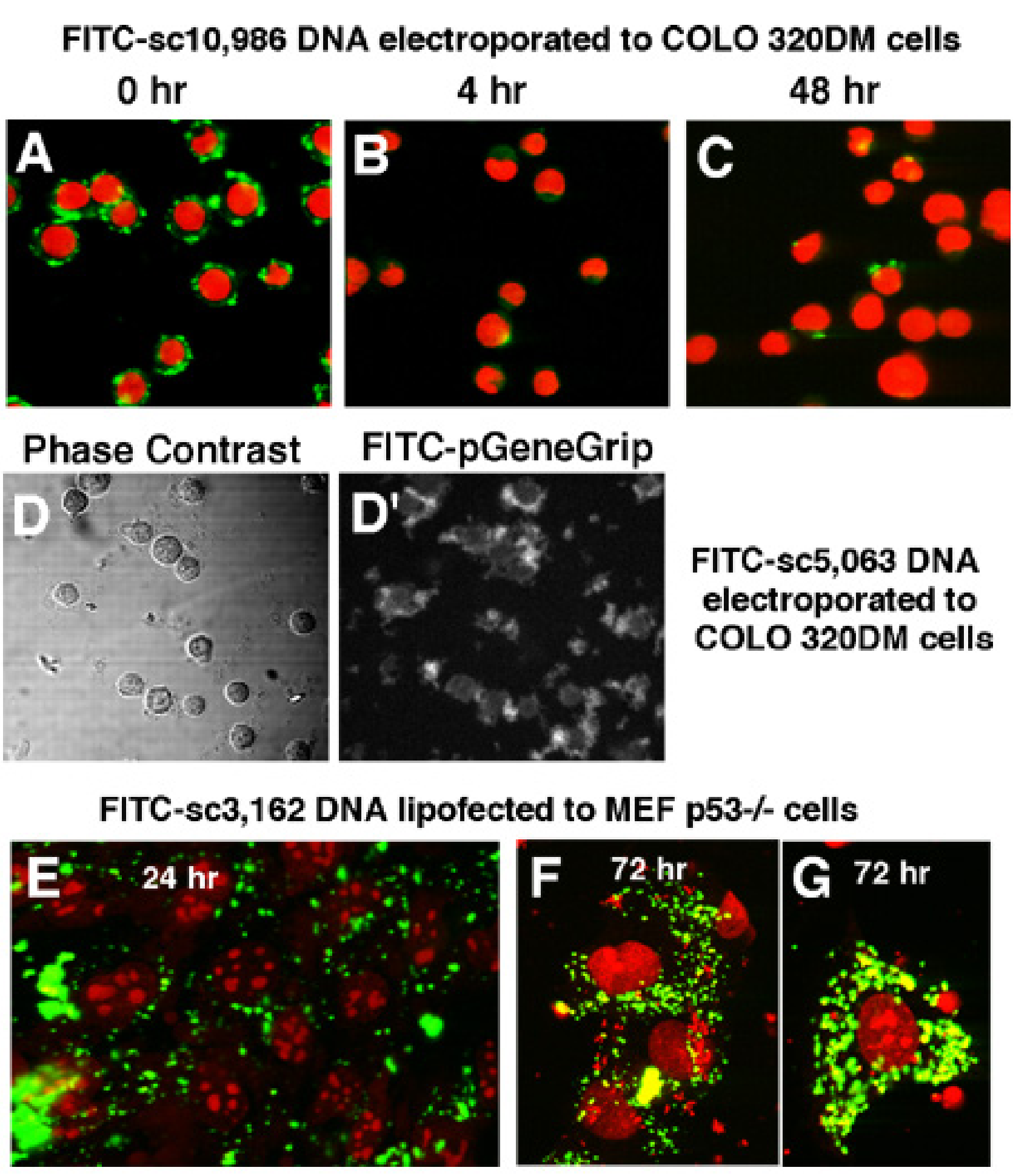
FITC-sc10,986 DNA electroporated to COLO 320DM cells
0 hr
4 hr
48 hr
A
B
C
Phase Contrast
FITC-pGeneGrip
D
D'
FITC-sc5,063 DNA electroporated to COLO 320DM cells
FITC-sc3,162 DNA lipofected to MEF p53-/- cells
E
24 hr
F
72 hr
G
72 hr

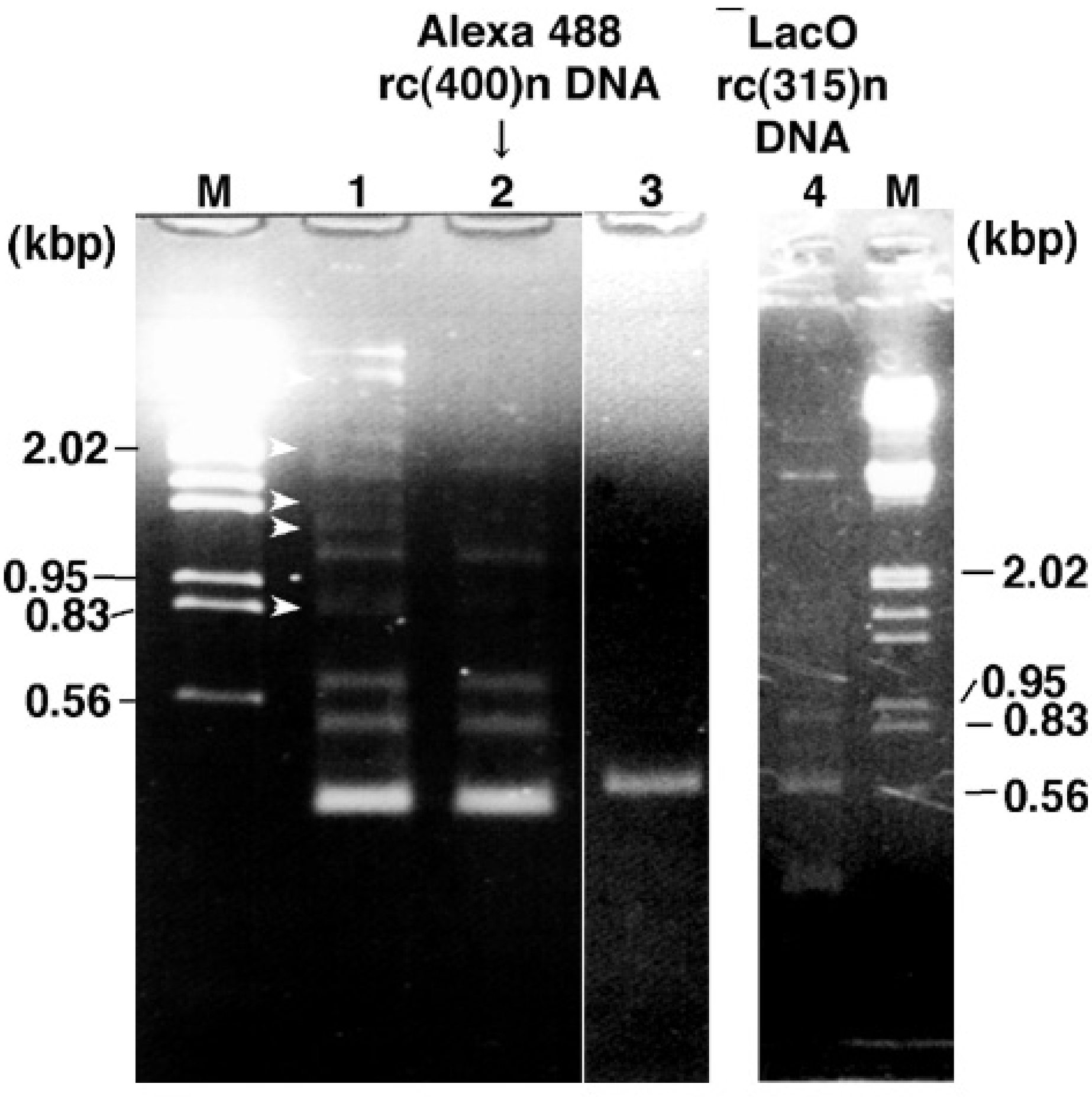
Alexa 488
rc(400)n DNA
LacO
rc(315)n
DNA
M
1
2
3
4
M
(kbp)
2.02
0.95
0.83
0.56
(kbp)
2.02
0.95
0.83
0.56

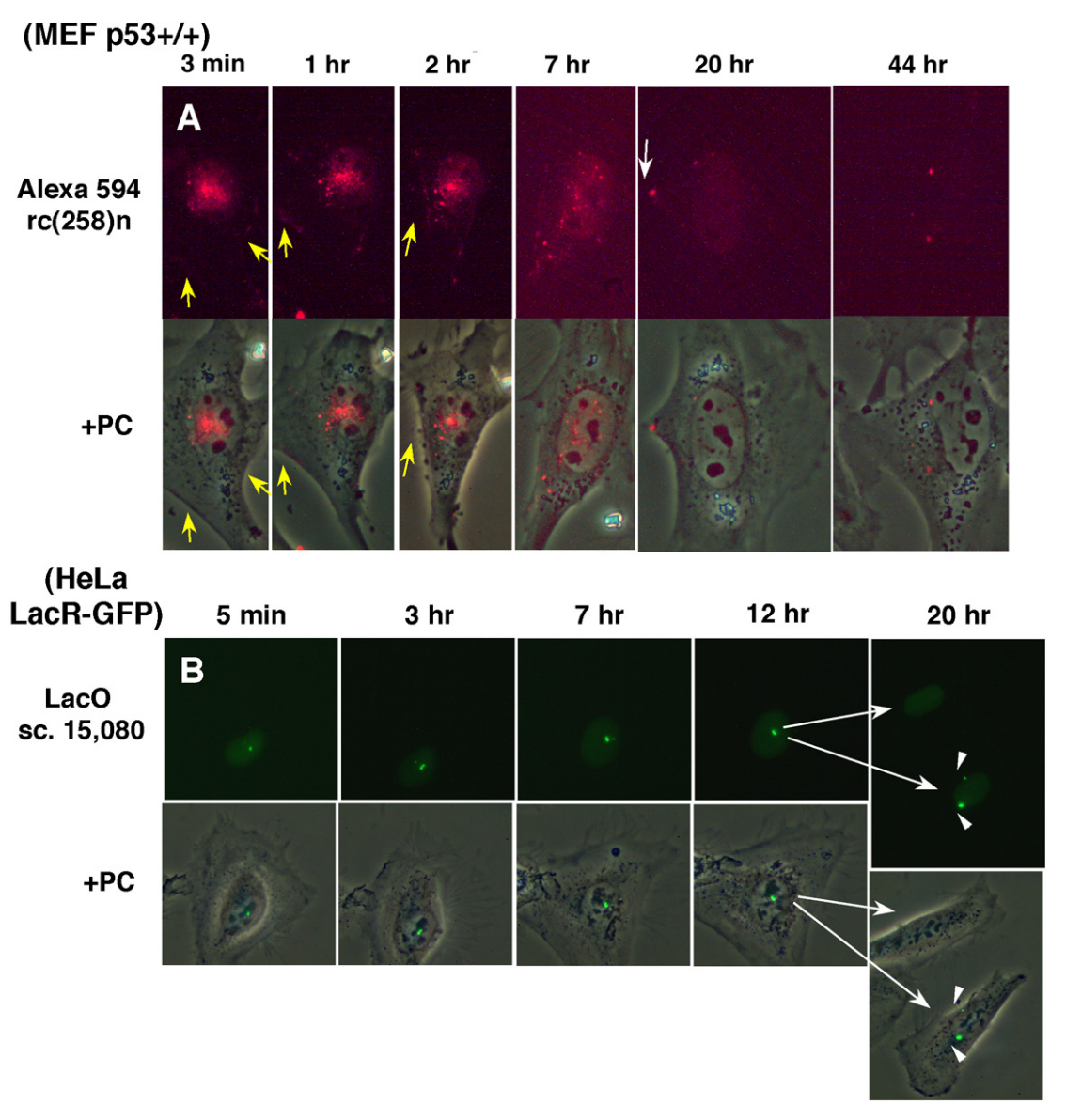
(MEF p53+/+)
3 min
1 hr
2 hr
7 hr
20 hr
44 hr
A
Alexa 594
rc(258)n
+PC
(HeLa
LacR-GFP)
5 min
3 hr
7 hr
12 hr
20 hr
B
LacO
sc. 15,080
+PC

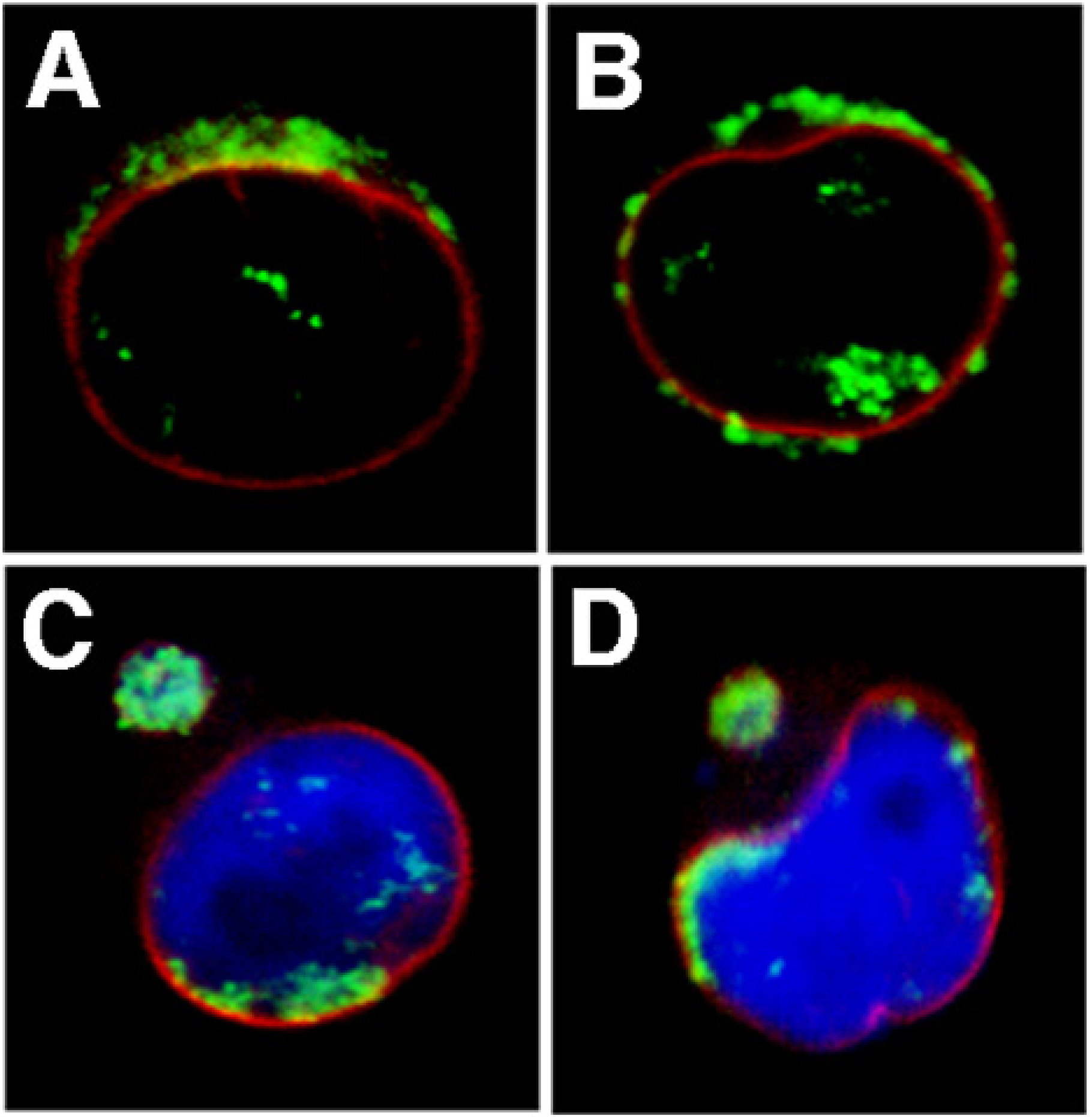
A
B
C
D